We are thankful to the reviewers and co-editor for their thoughtful and constructive comments on our study. The manuscript has been revised accordingly. Listed below is our point-to-point response to each comment.

Response to RC1

General comments:

The manuscript represents the results obtained by using a high-resolution time-of-flight aerosol mass spectrometer to monitor the chemical composition of submicron non-refractory aerosol at a high-altitude mountainous site at the edge of the Tibetan Plateau in China. The dominant component was found to be organic aerosol, with a contribution of 68%. Organic aerosol (OA) was found to be highly oxygenated and oxidized, depicting the secondary and processed nature of it. When deconvolving the organic aerosol to different factors, the two oxygenated factors, one originating from the processing of biomass burning and one highly oxidized, accounted for the 87% of the organic aerosol. The rest was identified as biomass burning organic aerosol (BBOA) originating from long-range transport both from neighboring countries (Myanmar) but also from nearby activities, exhibiting different degrees of processing according to its provenance. Concentrations of OA during the biomass burning influence were significantly higher than those during background conditions, denoting the important influence of long-range transport pollution at remote areas of the globe. Overall the manuscript is interesting and easy to follow. It focuses on an area of the globe that is not extensively studied, adding value to the reported results. Additionally, it demonstrates the importance of the influence from polluted areas to remote background sites situated away from local sources. Nevertheless there are some important details missing and more thorough discussion should be made in specific sections. Other than that the paper can be recommended for publication after addressing the issues listed below.

Specific comments:

Q1: It is listed in the measurements section (2.2) that a 7-wavelegth aethalometer was also collocated at the site. Based on the approach of Sandradewi et al. (2008) a source apportionment of the black carbon (BC) measurements could be effectuated for the distinction between a wood burning and a fossil fuel component. This could significantly increase the confidence in the identification of the biomass burning events and could possibly improve the correlations between the time series of OOA-BB and BBOA with BC. Since the measurements are there, it is a pity not to take advantage of all the information.

Reply: We thanks the reviewer for the comment. It would be nice to be able to separate the fossil fuel component from the wood burning component, however in our study, the approach of Sandradewi et al. (2008) could not be a valid method. The approach needs accurate parameterization of αTR for traffic and αWB for wood burning, which can only be obtained when measurements were done near the sources. In the case of our study, as the BC underwent the transportation process, it got coated, thus its AAE decreased (Chung et al., 2012). Most of the BC measured at the site was from transportation, thus gives us big uncertainties on the αTR and αWB values. Besides, the measurement was taken at a high mountain

site, with the nearest city located 20 km to the south, and more than 1000 m below its altitude. The air masses were mainly from the west or southwest of the site, covering mostly remote areas. Thus the traffic source should play a minor role in this study.

Q2: In the same section (2.2) it is stated that a Scanning Mobility Particle Sizer (SMPS) was used to measure the size distributions during the measurement campaign. How did the integrated mass from the SMPS compare to the added masses from the AMS and BC measurements?

Reply: We thank the reviewer for this question. We have done this comparison, and is shown in Figure S1 in the supplementary materials part of this manuscript.

Other minor comments:

L36: with their radiative forcing ..

Reply: Revised.

L65: convincing evidence ..

Reply: Revised.

L66: Most of the previous studies ..

Reply: Revised.

L84: making it an ideal site ..(delete "to be")

Reply: Revised.

L157: showed the highest probability ..

Reply: Revised.

L167: elemental composition was calculated ..

Reply: Revised.

L173: oxygenated fraction (instead of "oxygen")

Reply: Revised.

L207: It is stated that the OOA-BB of the study correlated well with aged BBOA from 3 hours downwind of a forest fire. Yet, in L214 it is noted that m/z 60 is reduced after long periods of atmospheric processing. This is somehow contradictory as 3 hours seems quite quick. Similar to the observations of the current study, Minguillón et al. (2015) identified a quite oxygenated factor (named OOAm from mix) which was partially made up from processed BBOA quite quickly and that explained the fact that the time series of OOA tracked that of the BBOA. Therefore it is suggested to rephrase L214 as to reflect the quick nature

77 of this processing.

78 Reply: We thank the reviewer for the suggestion. We have revised Line 183 as follow.

79 "Compared with BBOA measured near sources, OOA-BB shows a higher oxygenated degree, with an

80 O/C of 0.85, and a lower fraction of m/z 60 (0.6%), as a result of the oxidation of primary levoglucosan-

81 type species (Jolleys et al., 2015). This oxidation process can be quick in elevating the oxidation state

82 and reducing f_{60} (calculated as the ratio of the signal at m/z 60 to the total OA signal), which is also

83 reported in another study by Minguillón et al. (2015)."

84 L254: Replace "It includes" maybe with "Among other"

85 Reply: We thank the reviewer for the suggestion. The sentence in Line 220 is revised as follow: "with

86 the following criteria satisfied, i.e. (a) back…"

87

88 L257: from the south part ..

89 Reply: Revised.

90

91 L272: OA are represented by the left axis while other species are "represented" by the right axis.

92 Reply: Revised.

93

94 L275: were 10, 4 and 6-fold higher ..

95 Reply: Revised.

96

97 L278: remained low ..

98 Reply: Revised.

99

100 L282: Air mass or air masses (as mentioned before in the text)? Be consistent.

101 Reply: Revised.

102

103 L287: which could emit   ..

104 Reply: Revised.

105

106

107

108

109

110

111

112

113

114

115

Response to RC2

General comments:

This paper reports the chemical composition of submicron non-refractory aerosol at Mt. Yulong, a mountainous site at the southeast edge of the Tibetan Plateau in China, by using a high-resolution time-of-flight aerosol mass spectrometer, with other instruments such as aethalometer, SMPS, GC-MS/FID. The aerosol at Mt. Yulong was dominant by organic aerosol, following by sulfate, BC. The manuscript paid more attention to deconvolve the organic aerosol into three factors, i.e. biomass-burning organic aerosol (BBOA), BBOA, biomass-burning-influenced oxygenated organic aerosol (OOA-BB) and oxygenated organic aerosol (OOA). OOA-BB and OOA accounted for about 87% of organic aerosol, which suggests that the OA is highly oxygenated in this remote site. This study also points out that the southeastern edge of the Tibetan Plateau is affected by transport of anthropogenic aerosols from Southeast Asia. This work will add some understanding of the influence of biomass burning on remote site of Tibetan Plateau. The manuscript could be accepted for publication after revision.

Specific comments:

Q1: The authors mentioned in abstract": : :is affected by transport of anthropogenic aerosols from Southeast Asia." In fact, according to the back-trajectory, the aerosols were from South Asia, not Southeast Asia. Please check.

Reply: We thank the reviewer for the comment. We have revised "Southeast Asia" to "South Asia" in the title and in the manuscript.

Q2: In section "Measurements and data processing", the authors should add more information about AMS size calibration, what the CE value were used, what the AMS data time resolution for data collection and later analysis were.

Reply: We thank the reviewer for the comment. We have revised section 2.2 "Measurements and data processing" with the information added in Line 82 and Line 91 as follow.

"The time resolution was 5 min for AMS measurement, with 2.5 min in V mode to obtain mass concentration, and 2.5 min in W mode for HR mass spectrum of organics."

"In this study, the collection efficiencies varied from 0.5 to 0.9."

Q3: In Fig.S1, the mass concentration of PM_1 measured by SMPS and that of AMS plus Aethalometer has compared. The authors mentioned the estimated composition-dependent density was used. Please add what the value of aerosol density used?

Reply: We thank the reviewer for the question. We have added this information regarding aerosol densities in the supplementary materials part by adding the following sentence in SI Line 21:

"The aerosol density used was 1.4 g cm^{-3} for organics (Gysel et al., 2007), 1.75 g cm^{-3} for sulfate, nitrate and ammonium, and 1.80 g cm^{-3} for black carbon as suggested by Middlebrook et al. (2012)."

Q4：Biomass burning event 2 is different with the others, the contribution of BBOA is comparable to the background period. It would be better to have more evidence to support the explanation.

Reply: We thank the reviewer for the comment. We have added the following sentences in Line 245 – Line 246:

"Although the ratio of BBOA to the total OA during this event has a similar level to the background level, the mass concentrations of both OA and BBOA were more elevated than the background level."

Q5: Pearson Correlation Coefficient has mentioned many times in this manuscript, as we know, this value is related with the data points, please make them clear.

Reply: We thank the reviewer for the comment. We have added the number of data points at places where we mentioned the Pearson R values.

Q6: Line 80 Mt. Yulong (27.2oN, 100.2oE)

Reply: Revised.

Q7: the authors mentioned "particle number size distribution for particle mobility diameters ranging from 3 to 780 nm, In Table S1 just list 3081DMA and CPC 3775? Do you use two SMPS in parallel or not?

Reply: We thank the reviewer for the comment. We have modified in Line 96: "… 3 – 780 nm…" to "… 15 – 760 nm…", and have revised Table S1 as the follow.

"SMPS (3081-DMA and 3022-CPC)"

Q8: The carbonaceous species were very abundant in: : :", Carbonaceous species should include BC. Please rewrite this sentence.

Reply: We thank the reviewer for the comment. It is revised in Line 263 as follow: The carbonaceous species (OA+BC) were very abundant in PM_1, with an average contribution of 77%, followed by sulfate (14%) and ammonium (5%).

Q9: Line 567, the authors mentioned the axis for different species in the text, but not in the figure caption, please make the figure self-readable.

Reply: We thank the reviewer for the suggestion. It is revised in Line 498: Organic aerosols are represented by the left axis while other species are represented by the right axis.

193   Reference

194   Chung, C. E., Kim, S. W., Lee, M., Yoon, S. C., and Lee, S.: Carbonaceous aerosol AAE inferred from

195   in-situ aerosol measurements at the Gosan ABC super site, and the implications for brown carbon aerosol,

196   Atmospheric Chemistry and Physics, 12, 6173-6184, 10.5194/acp-12-6173-2012, 2012.

197   Gysel, M., Crosier, J., Topping, D. O., Whitehead, J. D., Bower, K. N., Cubison, M. J., I.Williams, P.,

198   Flynn, M. J., McFiggans, G. B., and Coe, H.: Closure study between chemical composition and

199   hygroscopic growth of aerosol particles during TORCH2, ACP, 7, 6131-6144, 10.5194/acp-7-6131-2007,

200   2007.

201   Jolleys, M. D., Coe, H., McFiggans, G., Taylor, J. W., O'Shea, S. J., Breton, M. L., Bauguitte, S. J.-B.,

202   Moller, S., Carlo, P. D., Aruffo, E., Palmer, P. I., Lee, J. D., Percival, C. J., and Gallagher, M. W.:

203   Properties and evolution of biomass burning organic aerosol from Canadian boreal forest fire, Atmos.

204   Chem. Phys., 15, 3077-3095, 10.5194/acp-15-3077-2015, 2015.

205   Middlebrook, A. M., Bahreini, R., Jimenez, J. L., and Canagaratna, M. R.: Evaluation of Composition-

206   Dependent Collection Efficiencies for the Aerodyne Aerosol Mass Spectrometer using Field Data,

207   Aerosol Sci. Technol., 46, 258-271, 10.1080/02786826.2011.620041, 2012.

208   Minguillón, M. C., Ripoll, A., Pérez, N., Prévôt, A. S. H., Canonaco, F., Querol, X., and Alastuey, A.:

209   Chemical characterization of submicron regional background aerosols in the western Mediterranean

210   using an Aerosol Chemical Speciation Monitor, Atmospheric Chemistry and Physics, 15, 6379-6391,

211   10.5194/acp-15-6379-2015, 2015.

212   Sandradewi, J., Prévôt, A. S. H., Szidat, S., Perron, N., Alfarra, M. R., Lanz, V. A., Weingartner, E., and

213   Baltensperger, U.: Using Aerosol Light Absorption Measurements for the Quantitative Determination of

214   Wood Burning and Traffic Emission Contributions to Particulate Matter, Environ. Sci. Technol., 42,

215   3316–3323, 2008.

216

217

218

219

220

221

222

223

224

225

226

227

228

229

230

231

232

233

234

235

236

237   Response to co-editor:

238   Please add some technical details in sections 2.2 and 2.3 before uploading your files for production.

239   In section 2.2

240   - Manufacturers of AMS, SMPS, Aethalometer, GC-MS/FID, etc.

241   Reply: We thank the editor for the comment. The information about manufacturers of each instrument

242   has been added in Line 80, 95 and 97. The details of main instruments are shown in Table S1 in the

243   supplementary materials part of this manuscript.

244

245   In section 2.3

246   - URL for the WRF model.

247   - What model was used for calculating back trajectories? What meteorological data were used for the

248   calculations? Links should also be provided for both.

249   Reply: We thank the editor for the question. We have revised section 2.3 with the information added in

250   Line 107 and Line 109 as follow:

251   … the Weather Research and Forecasting (WRF) model (version 3.61, www.wrf-

252   model.org/index.php) ...

253   The original data for WRF model are available from National Centers for Environmental Prediction

254   (NCEP) Final (FNL) Operational Global Analysis data (http://rda.ucar.edu).

Influence of biomass burning from South Asia at a high-altitude mountain receptor site in China

Jing Zheng[1], Min Hu[1,*], Zhuofei Du[1], Dongjie Shang[1], Zhaoheng Gong[2,a], Yanhong Qin[1], Jingyao Fang[1], Fangting Gu[1], Mengren Li[1], Jianfei Peng[1], Jie Li[3], Yuqia Zhang[3], Xiaofeng Huang[2], Lingyan He[2], Yusheng Wu[1], Song Guo[1]

[1]State Key Joint Laboratory of Environmental Simulation and Pollution Control, College of Environmental Sciences and Engineering, Peking University, Beijing, China

[2]Key Laboratory for Urban Habitat Environmental Science and Technology, School of Environment and Energy, Peking University Shenzhen Graduate School, Shenzhen, China

[3]State Key Laboratory of Atmospheric Boundary Layer Physics and Atmospheric Chemistry (LAPC), Nansen-Zhu International Research Center (NZC), Institute of Atmospheric Physics, Chinese Academy of Sciences, Beijing, China

* *Correspondence to*: minhu@pku.edu.cn

[a] Now at John A. Paulson School of Engineering and Applied Sciences, Harvard University, Cambridge, Massachusetts, 02138, United States

Abstract

Highly time-resolved in-situ measurements of airborne particles were made at Mt. Yulong (3410 m above sea level) on the southeastern edge of the Tibetan Plateau in China from 22nd March to 14th April in 2015. Detailed chemical composition was measured by a high-resolution time-of-flight aerosol mass spectrometer together with other online instruments. Average mass concentration of the submicron particles (PM_1) was 5.7 ± 5.4 μg m^{-3} during the field campaign, ranging from 0.1 μg m^{-3} up to 33.3 μg m^{-3}. Organic aerosol (OA) was the dominant component in PM_1, with a fraction of 68 %. Three OA factors, i.e., biomass-burning organic aerosol (BBOA), biomass-burning-influenced oxygenated organic aerosol (OOA-BB) and oxygenated organic aerosol (OOA), were resolved using positive matrix factorization analysis. The two oxygenated OA factors accounted for 87 % of the total OA mass. Three biomass burning events were identified by examining the enhancement of black carbon concentrations and the f_{60} (the ratio of the signal at m/z 60 from the mass spectrum to the total signal of OA).

Back trajectories of air masses and satellite fire map data were integrated to identify the biomass burning locations and pollutants transport. The western air masses from South Asia with active biomass burning activities transported large amount of air pollutants, resulting in elevated organic concentrations up to 4-fold higher than that of the background condition. This study at Mt. Yulong characterizes the tropospheric background aerosols of the Tibetan Plateau during pre-monsoon season, and provides clear evidence that the southeastern edge of the Tibetan Plateau was affected by transport of anthropogenic aerosols from South Asia.

1 Introduction

Aerosols play an important role in the radiative balance in earth's atmosphere, with their radiative forcing still having large uncertainties (IPCC, 2013). Biomass burning emission is one of the dominant sources of atmospheric particles (von Schneidemesser et al., 2015), contributing up to 90 % of the primary organic aerosol in the global scale (Bond et al., 2004) and more than half of the total organic aerosol mass in areas with significant biomass burning influences (e.g. Yangtze River Delta region in China, and Indian Peninsula) (Zhang et al., 2015;Engling and Gelencser, 2010). Given the long atmospheric lifetime of aerosols, even remote areas can sometimes be influenced by the transportation of air pollutants from areas with active biomass burnings (Bougiatioti et al., 2014). In terms of the deterioration of air quality and climate change in those remote areas, great scientific interest has arisen focusing on the impacts on biomass burning (Lau et al., 2010;Qian et al., 2011).

The Tibetan Plateau is the largest and highest plateau in the world, and is often regarded as the "Third Pole". It is surrounded by a ring of high-elevated mountain ranges, which were considered as blocks for transportations of air pollutants from its vicinity (Wang and French, 1994). Since this vast land has a relatively low population density with minor anthropogenic influences, the Tibetan Plateau has been considered as a natural background of the Eurasian continent (Ming et al., 2010;Wan et al., 2015). In recent years, studies have presented convincing evidence for the transport route of air pollutants climbing over the Himalayas, especially during pre-monsoon season, coinciding with the annual intensive fire season in South and Southeast Asia (Streets et al., 2003;Marinoni et al., 2010;Cong et al., 2015b). A westerly dry circulation helps to build up the smoke

plume against the Himalayan ridges, elevating to 3-5 km in altitude (Bonasoni et al., 2010;Xia et al., 2011). Subsequently, downward glacier wind of local mountain breeze circulation brings biomass burning related air pollutants down to the mountain valley (Cong et al., 2015b;Lüthi et al., 2015).

A host of studies based on field campaigns have amassed an impressive amount of information describing the biomass burning influence on different areas of the Tibetan Plateau (Decesari et al., 2010;Zhao et al., 2013;Xu et al., 2015). Those studies were mostly approached by analyzing the temporal and spatial variations of atmospheric composition based on filter measurements. The strong correlation of carbonaceous aerosol with biomass burning tracers K^+ and levoglucosan pointed out the origins of aerosols (Cong et al., 2015a). Biomass burning organic aerosol (BBOA) was also found to be a major fraction of organic aerosol (OA), with a 15 % contribution to the total OA mass (Du et al., 2015). Xu et al. (2013) and You et al. (2016) also presented convincing evidence about biomass burning impacts by analyzing chemical components in glaciers collected in the Tibetan Plateau. Most of previous studies were based on offline analysis using filter or glacier samples, which were limited to low time resolution, making it difficult to follow the aging process of biomass burning aerosol. Thus in-situ measurements of aerosol chemical characterization with high time resolution are needed, so as to have a deep understanding of the sources and evolution of the particulate matter.

In this study, the influence of biomass burning from South Asia on the Tibetan Plateau has been analyzed. The results can serve as inputs or constraints for global climate model simulations. By examining the aerosol properties as a function of chemical composition at Mt. Yulong at the southeastern edge of the Tibetan Plateau, this study sheds light on the evolution processes of OA. Positive matrix factorization analysis has been conducted to resolve different sources of OA. And the influence of biomass burning from South Asia transported over long distances to the Tibetan Plateau background environment during pre-monsoon season has been characterized.

2 Method

2.1 Site description and meteorological conditions during the campaign

In this study, we conducted an intensive observation at the site on Mt. Yulong (27.2 °N, 100.2 °E), with an altitude of 3410 m a.s.l., northwestern Yunnan Province, China (Fig. 1). Since Mt. Yulong is lying in the transition zone extending from the low altitudes of the Yunnan Plateau (~ 3000 a.s.l.) to the high altitude of the Tibetan Plateau (~ 5000 a.s.l.), it is on the transport route of pollutants from South Asia to inland China, making it an ideal site to observe the influence of regional and long-range transport of polluted air masses. This station is a member of the National Atmospheric Watch Network coordinated by the Chinese Environmental Monitoring Center. The famous tourist attraction Lijiang Old Town locates more than 20 km away and 1000 m lower than the elevation of the station. The observation period was conducted during the pre-monsoon season of the Tibetan Plateau, from 22nd March to 14th April 2015, corresponding to the annual biomass burning seasons in South Asia. Since the season was cold with sparse visitors in Lijiang old city, the influence of local emissions from residents and visitors remained low compared with other seasons.

2.2 Measurements and data processing

A high resolution time-of-flight aerosol mass spectrometer (AMS, Aerodyne Research Inc.) was deployed to measure the highly time-resolved chemical composition of sub-micron, non-refractory aerosols (Table S1). The standard operation procedures of the AMS has been described in detail in Canagaratna et al. (2007). The time resolution was 5 min for AMS measurement, with 2.5 min in V mode to obtain mass concentration, and 2.5 min in W mode for HR mass spectrum of organics. The detection limits (DL) of organic, sulfate, nitrate, ammonium and chloride were 0.07, 0.004, 0.003, 0.005 and 0.01 $\mu g\ m^{-3}$, respectively. During most time of the campaign, the mass concentrations of chloride were below its DL, and including it would lower the total signal to noise ratio, therefore it is omitted from the analysis.

The AMS data was analyzed using the standard AMS data analysis software, i.e., SQUIRREL (version 1.57) for unit resolution mass spectrum data, and PIKA (version 1.16) for high resolution mass spectra data. Calibrations of the AMS on

4

89 flow rate and ionization efficiency were conducted each week. To account for the particle loss due to the bounce of particles

90 on the vaporizer, collection efficiencies were calculated and applied for data correction based on the method described by

91 Middlebrook et al. (2012). In this study, the collection efficiencies varied from 0.5 to 0.9.

92   The high resolution organic aerosol spectra were further apportioned to different sources by positive matrix factorization

93 (PMF) analysis (Paatero and Tapper, 1994;Ulbrich et al., 2009). The solution was validated by the characteristics of resolved

94 mass spectra, as well as the comparison of temporal variations between each factor and external species (e.g. acetonitrile).

95   Other online instruments were also deployed at the site (Table S1). A scanning mobility particle sizer (SMPS, TSI Inc.) was

96 used to measure particle number size distribution for particle mobility diameters ranging from 15 to 760 nm, with a time

97 resolution of 5 min. An Aethalometer (Magee Scientific) was deployed to measure the aerosol light absorption coefficients σ_{ap}

98 at its seven wavelengths, ranging from 370 to 950 nm. Black carbon (BC) concentration is determined by σ_{ap} at 880 nm using

99 the default mass attenuation cross sections of 16.6 m^2 g^{-1} (Fröhlich et al., 2015). Acetonitrile was measured by a gas

100 chromatographer with mass spectrometer and flame ionization detectors (GC–MS/FID) with a time resolution of 1 hour.

101 Technical details of this self-made instrument were described elsewhere (Wang et al., 2016).

102   Meteorological parameters, including relative humidity, temperature, wind direction and wind speed, were continuously

103 monitored on the site during the campaign. The low temperature (5 ℃ for the whole campaign average) and heavy snow

104 eliminated the influence of biogenic emissions to this site during the campaign.

105 **2.3 Back trajectory analysis and fire maps**

106   To explore the influence of regional biomass burning activities on aerosol properties during the campaign, the Weather

107 Research and Forecasting (WRF) model (version 3.61, www.wrf-model.org/index.php) was used to investigate the

108 meteorological conditions and to compute trajectories of air masses arriving at Mt. Yulong. The original data for WRF model

109 are available from National Centers for Environmental Prediction (NCEP) Final (FNL) Operational Global Analysis data

110 (http://rda.ucar.edu). 48-h back trajectories were calculated every 6 hours from March 22nd to April 14th, using a starting

111   height at 600 m above the ground level of the site.

112   Active fire points were obtained from the Fire Information for Resource Management System (FIRMS), which is provided

113   by the Moderate Resolution Imaging Spectroradiometer (MODIS) satellite (https://firms.modaps.eosdis.nasa.gov/firemap/,

114   last accessed on Aug. 26, 2016).

115   3 Results

116   3.1 Concentrations and chemical compositions of submicron aerosols

117   The time series of submicron aerosol compositions as well as meteorological conditions are shown in Fig. 2. The average

118   PM_1 concentration was 5.7 ± 5.4 µg m^{-3}, with a range of 0.1 µg m^{-3} – 33.3 µg m^{-3}. This result was similar to previous

119   observations at the Northern Tibetan Plateau, where Du et al. (2015) reported an average PM_1 concentration of 11.4 µg m^{-3} in

120   the autumn of 2013, and Xu et al. (2014a) reported an annual average $PM_{2.5}$ concentration of 9.5 µg m^{-3} from 2006 to 2007.

121   The averaged PM_1 concentration was much lower than those measured at urban and downwind sites of China (e.g., Huang et

122   al., 2013;Xu et al., 2014b), but was three times higher than the 1.7 µg m^{-3} at a background site in Europe in March 2004

123   (Sjogren et al., 2008), and ten times higher than that measured at the same background site in the spring of 2013 (Fröhlich et

124   al., 2015). These huge differences indicate that anthropogenic pollutions in South Asia may have resulted in the elevation of

125   aerosol concentrations to levels above the natural background level.

126   Averaged aerosol composition of PM_1 is shown in the pie chart (Fig. 3(a)). The PM_1 chemical composition was dominated

127   by organic components, which accounted for 68 %, followed by sulfate (14 %). The minor contribution of nitrate to PM_1 (4 %)

128   can be explained by the lack of nearby anthropogenic sources for precursors (e.g., HONO, N_2O_5) (Du et al., 2015). This result

129   presents a similar picture as those observed at remote sites in the northern hemisphere (Zhang et al., 2011), as well as at a high

130   altitude site in Europe (Ripoll et al., 2015). Compared with urban or regional areas in China, where secondary inorganic species

131   including sulfate, nitrate and ammonium typically contribute to over one half of the total mass concentrations, the result at this

132   site is quite unique (Huang et al., 2010;Huang et al., 2012;Xu et al., 2014b).

Figure 3(b) shows the relative contribution of major chemical components as a function of PM_1 mass concentrations, as well as the probability density of PM_1 mass loading. PM_1 concentrations below 5 μg m^{-3} showed the highest probability (68 %). The fractions of organics and BC increase slightly with the increasing of PM_1 concentrations, showing that they were the main contributors to the pollution episodes in Mt. Yulong.

The PM_1 components did not show distinct diel variations, but remained relatively constant during the whole day, as shown in Fig. 3(c). This is similar to the findings at the Puy-de-Dôme station in central France, and the Montsec station in western Mediterranean Basin (Freney et al., 2011;Ripoll et al., 2015). Strong long-range transport of air masses with few local emissions could blur the diel cycles, since the air-mass transportations occurred regardless of the local time of the day.

3.2 Characterization of organic aerosol

3.2.1 Elemental compositions of organic aerosol

The elemental composition was calculated from high resolution mass spectra of organics obtained by AMS, using the method developed by Canagaratna et al. (2015). Compared with the previous method (Aiken et al., 2007;2008), the ratio of O/C and H/C are typically increased by 20 % and 7 %, respectively. Bulk OA was mainly composed of carbon and oxygen, with minor contributions from hydrogen and nitrogen, and had an average molecular formula of $C_1H_{1.4}O_{1.1}N_{0.04}$. The fragments of organics were grouped into five types according to the existence of C, H, O or N atoms. $C_xH_y^+$ were only 21 % of the total organic signal, while the oxygenated fraction ($C_xH_yO_z^+$) accounted for 68 % of the total OA, which is higher than those measured at urban and downwind site (30-41 %) (Huang et al., 2011;Sun et al., 2011;Hu et al., 2013). The average OM/OC and O/C ratios for the whole campaign were 2.63 and 1.11, respectively, and were similar to those measured in the north eastern region of the Tibetan Plateau (OM/OC 2.75, O/C 1.16) (Xu et al., 2015). These results are slightly higher than the elemental ratios measured at another remote site (OM/OC: 2.4, O/C: 0.9) in the eastern Mediterranean (Bougiatioti et al., 2014), probably due to the mixture of free troposphere aerosol after a long time of processing before arriving at this high altitude site. The extremely high value of OM/OC reflects the highly oxidized nature of OA in the Tibetan Plateau.

3.2.2 Source apportionment of organic aerosol

PMF analysis was performed to investigate the sources of OA measured at Mt. Yulong. Three factors were resolved, including a biomass burning organic aerosol (BBOA), an oxygenated biomass-burning-influenced organic aerosol (OOA-BB), and an oxygenated organic aerosol (OOA). Details of the PMF analysis can be found in the supplement. The mass spectra of the three factors are shown in Fig. 4. The time series of the three factors and an external species (acetonitrile) are plotted in Fig. 5.

3.2.2.1 BBOA

BBOA has been frequently identified in previous studies at urban and regional sites (Zhang et al., 2011). The mass spectrum of BBOA has a notable contribution from m/z 60 (mainly $C_2H_4O_2^+$, contributing 3.1 % of the total mass spectra), which is from fragmentation of levoglucason. As shown in Table 1, the mass spectrum correlates well with the samples from an aircraft measurement above a large forest fire (Brito et al., 2014), and well with the samples from biomass burning simulation system in the laboratory (He et al., 2010). BBOA has an O/C ratio of 0.37, presenting a similar level to previous studies (Aiken et al., 2008;He et al., 2010). The time series of BBOA correlates very well with K^+ based on filter analysis (Pearson R=0.92, N=13). The factor was also confirmed to be BBOA, since it has a similar temporal variation to that of acetonitrile (Fig. 5), a gas phase tracer for biomass burning.

The average concentration of BBOA was 0.5 μg m^{-3} for the whole campaign, accounting for 13 % of the total OA mass, with a maximum contribution at 61 % (Fig. 6 (a)). The spikes in the time series of BBOA indicate that a fraction of BBOA was contributed by primary sources nearby, possibly occasional biomass burning activities for domestic heating and cooking. The increasing fraction of BBOA as a function of total OA concentrations points to contributions from biomass burning activities during the pollution episodes (Fig. 6 (b)).

3.2.2.2 OOA-BB

The mass spectrum of OOA-BB factor was dominated by $C_xH_yO_z^+$ fragments, especially org29 (CHO$^+$), org43 ($C_2H_3O^+$) and org44 (CO$_2^+$). The spectrum of OOA-BB in this study well correlated with aged BBOA obtained 3 hours downwind of a

178 forest fire (Brito et al., 2014) (Pearson R=0.97, N=100). It is qualitatively similar to published OOA-BB spectra from aged

179 BB plumes in China during the harvest seasons (Zhang et al., 2015), and also presented many similarities to those of OOA2-

180 BBOA resolved in the metropolitan area of Paris (Crippa et al., 2013).

181 The average concentration of OOA-BB was 0.9 µg m^{-3} for the whole campaign, accounting for 22 % of the total OA mass.

182 Compared with BBOA measured near sources, OOA-BB shows a higher oxygenated degree, with an O/C of 0.85, and a

183 lower fraction of m/z 60 (0.6 %), as a result of the oxidation of primary levoglucosan-type species (Jolleys et al., 2015). This

184 oxidation process can be quick in elevating the oxidation state and reducing f_{60} (calculated as the ratio of the signal at m/z 60

185 to the total OA signal), which is also reported in another study by Minguillón et al. (2015). As the plumes originated from

186 South Asia were measured at a distance of several hundred kilometers downwind, emissions would have undergone

187 substantial aging prior to sampling. The aging process includes both the gas-phase oxidation of semi volatile species from

188 biomass burning sources and heterogeneous or homogeneous reactions of existing particles during long-range transport

189 (Bougiatioti et al., 2014). The time series of OOA-BB and BBOA yield modest correlations with BC (Pearson R=0.62 and

190 0.65, N=5940). If we focus on the total biomass burning related organic aerosols (OOA-BB + BBOA), the R value for its

191 correlation with BC would increase to 0.76 (N=5940), indicating biomass burning related OA originated from the same

192 source as BC.

193 3.2.2.3 OOA

194 OOA is described as highly oxidized, aged particles formed after long-range transportation and processing. The mass

195 spectral properties of OOA are defined by having a dominant peak at m/z 44 (mainly CO_2^+) and other ions of $C_xH_yO_z^+$. The

196 highly oxidized nature of OOA is also reflected by its high O/C ratio of 1.45. The mass spectrum of OOA resembles that of

197 more oxidized OOA (MO-OOA) in Beijing well (Pearson R=0.69, N=100) (Hu et al., 2016).

198 OOA has an average concentration of 2.6 µg m^{-3}, accounting for 65 % of the total OA mass. Unlike previous studies at urban

199 or regional sites (Jimenez et al., 2009;Li et al., 2015;Hu et al., 2016), the time series of OOA did not agree well with that of

200 sulfate (Pearson R=0.32, N=5940), which was also the case at the puy-de-Dome research station (1465 m a.s.l.) (Freney et al.,

9

201 2011). The low Pearson correlation value can be partially explained by the extremely high concentration of OOA formed from

202 the oxidation of organics emitted by biomass burning activities during the first week of the campaign. For the rest of campaign,

203 the correlation value for sulfate with respect to OOA factor increased to 0.79 (N=3878), which is consistent with previous

204 studies.

205   As shown in Fig. 6(a), the two OOA factors (OOA-BB and OOA) were very abundant, with a predominantly contribution

206 of 87 % to the total OA mass. This is consistent with the high oxygen level in the total OA. During 80 % of the observation

207 period, OA concentrations were lower than 5 $\mu g\ m^{-3}$, with strong contributions from secondary organic aerosols (OOA and

208 OOA-BB) (Fig. 6 (b)). This indicates that the background site was predominated by organic aerosols formed through regional

209 transportation.

210 **4 Discussion**

211 **4.1 Identification of biomass burning events**

212   Enhanced BC concentrations were used to help identifying periods influenced by biomass burning plumes (Bougiatioti et

213 al., 2014). The BC concentration of 85 ng m^{-3} was taken as the background concentration at this site. It is the average

214 concentration observed in the beginning of April (1st April to 4th April), when the strong wind scavenged pollutants of the

215 whole region. Back trajectory and fire maps illustrate that the dominant air masses for this period was from north India with

216 minor biomass burning activities (see Fig. 7(d)). This concentration is consistent with the two-year averaged background level

217 measured at Southern Himalayas (Marinoni et al., 2010), and comparable to the lowest BC concentrations found over the

218 southeastern Tibetan Plateau in the pre-monsoon season (Engling et al., 2011).

219   During the sampling period, three episodes were identified as being influenced by biomass burning, with the following

220 criteria satisfied, i.e. (a) Back trajectory analysis shows a uniform source region; (b) Fire map shows fire spots in the region

221 during the episode; (c) BC concentrations were higher than the background level of 85 ng m^{-3} determined above. One long-

222 lasting and strong episode was from 22nd March to 30th March. The air masses arrived at the site during this period were from

223   the north part of Myanmar, and covered active biomass burning areas (see Fig. 7(a)). As shown on the fire map, the site may

224   also be influenced by wildfires in the vicinity. Two less intense events were observed on 5th – 6th April and 11th – 12th April,

225   with slightly elevated BC concentrations. During the third event (11th – 12th April), the site experienced heavy snow. The

226   back trajectory shows that air masses to this region were transported from regions with few fire spots. The enhanced BC

227   concentration was probably emitted by biomass burning activities nearby for domestic heating and cooking.

228   These three biomass burning events were further validated by the increase of the fraction of biomass burning tracers, f_{60}.

229   During the first and second events, the average f_{60} were 0.98 % and 0.61 %, respectively. These values were much lower than

230   the f_{60} of 1.4 % during the third event, which was influenced by fires in the vicinity. This showed the decay of f_{60} in ambient

231   plumes transported from sources to the receptor site. During the clean episode, the f_{60} decreased to about 0.4 %, indicating

232   minor biomass burning influence (Cubison et al., 2011).

233   The box plot (Fig. 8) shows the concentrations of different chemical components of biomass burning events and background

234   conditions. The aerosol concentrations corresponding to the background condition is highlighted by light gray. Organic

235   aerosols are represented by the left axis while other species are represented by the right axis. Aerosols corresponding to biomass

236   burning events were at high concentrations. The concentrations of organic aerosol during three biomass burning events were

237   10, 4 and 6-fold higher than that of the background condition. During the first event, due to co-occurrence of biomass burning

238   activities in the vicinity together with the long-range transport of biomass burning plume, the concentration of BC reached 14

239   times higher than that of the background condition. All species remained low and sustained background concentrations during

240   the clean episode, with an average PM_1 concentration of 1.2 μg m^{-3}.

241   **4.2 Characteristic of three Biomass burning events**

242   The comparison of OA fractions of different biomass burning events is shown in Fig. 9. Since the air masses arriving at Mt.

243   Yulong during the second event were transported from active biomass burning areas in Myanmar within 48h, most of the

244   freshly emitted BBOA were processed and transformed to more oxidized OA, with OOA and OOA-BB together accounting

245   for 90 % on average of the total organic mass. Although the ratio of BBOA to the total OA during this event has a similar level

246   to the background level, the mass concentrations of both OA and BBOA were more elevated than the background level. In

247   contrast, the fraction of BBOA had strong enhancement during the third event, reaching 23 %. It is consistent with the

248   previously mentioned identification that the biomass burning plumes were mainly from residential heating nearby, which could

249   emit large amount of fresh BBOA.

250   The aging and/or mixing processes of different biomass burning plumes are further characterized in terms of the f_{44} vs. f_{60}

251   triangle plot (Cubison et al., 2011). f_{44}, similarly defined to f_{60} as the ratio of the signal at m/z 44 to the total OA signal, is used

252   here as an indicator of atmospheric aging, since OA and their gas phase precursors evolve in the atmosphere by becoming

253   increasingly oxidized with higher CO_2^+ fraction (Jimenez et al., 2009;Ng et al., 2010). BBOA can be clearly distinguished

254   from oxidized OA in the triangle plot. With the aging process of biomass burning plumes, OA evolved toward higher f_{44} and

255   lower f_{60}, and gained more similar signature with OOA.

256   The OA clusters of three biomass burning events are shown clearly in the f_{44}-f_{60} triangle plot (Fig. 10). The OA clusters of

257   the first and third events both present OA peaks with high f_{60} values, since the site was possibly influenced by residential

258   heating in the surrounding regions during these two episodes. The OA cluster of the second event presents more similar

259   oxidative properties to OOA and OOA-BB, due to loss of biomass burning marker through aging process during transport.

260   **5 Conclusions**

261   During the pre-monsoon season the aerosol evolution was explored at a high altitude receptor site on Mt. Yulong (3410 m

262   a.s.l.) in the Tibetan Plateau in Southwestern China. The average concentration of PM_1 was 5.7 μg m^{-3}, which was far below

263   that measured in urban and suburban as well as regional sites of China. The carbonaceous species (OA+BC) were very

264   abundant in PM_1, with an average contribution of 77 %, followed by sulfate (14 %) and ammonium (5 %). This high altitude

265   mountain site is suitable for tracing the influence of pollution plumes transported from the large areas of South Asia.

266   Using PMF analysis, organic aerosol was resolved into three factors, BBOA, OOA-BB and OOA. OOA-BB formed after

atmospheric process of BBOA during long-range transport. The two oxygenated OA factors (OOA and OOA-BB) accounted for 87 % of the total OA, showing the highly oxidized nature of aerosol at the Mt. Yulong.

Different types of biomass burning events were identified by examining organic tracer in mass profiles and BC concentrations. The origins of biomass burning plumes were verified by analyzing the back trajectories of air masses as well as fire maps. Elevated PM_1 concentrations due to the transport of air pollutants from active biomass burning areas in South Asia were observed. Domestic heating activity also had interference on the background condition of Mt. Yulong.

This study provides clear evidence on the influence of the transport of pollutants emitted by biomass burning activity in South Asia on the southeastern edge of the Tibetan Plateau in China. The chemical characteristics of aerosols observed by in situ measurement can serve as inputs for model validations of aerosol-cloud processes and long-range transports. This study also highlights the impact of anthropogenic emissions to the pristine region of the Tibetan Plateau, which may influence global climate.

6 Data availability

The data presented in this article are available from the authors upon request (minhu@pku.edu.cn).

References

Aiken, A. C., DeCarlo, P. F., and Jimene, J. L.: Elemental Analysis of Organic Species with Electron Ionization High-Resolution Mass Spectrometry, Anal. Chem., 79, 8350-8358, 10.1021/ac071150w, 2007.

Aiken, A. C., Decarlo, P. F., Kroll, J. H., Worsnop, D. R., Huffman, J. A., Docherty, K. S., Ulbrich, I. M., Mohr, C., Kimmel, J. R., Sueper, D., Sun, Y., Zhang, Q., Trimborn, A., Northway, M., Ziemann, P. J., Canagaratna, M. R., Onasch, T. B., Alfarra,

290 M. R., Prevot, A. S. H., Dommen, J., Duplissy, J., Metzger, A., Baltensperger, U., and Jimenez, J. L.: O/C and OM/OC Ratios
291 of Primary, Secondary, and Ambient Organic Aerosols with High-Resolution Time-of-Flight Aerosol Mass Spectrometry,
292 Environ. Sci. Technol., 42, 10.1021/es703009q, 2008.

293 Bonasoni, P., Laj, P., Marinoni, A., Sprenger, M., Angelini, F., Arduini, J., Bonafè, U., Calzolari, F., Colombo, T., Decesari, S.,
294 Di Biagio, C., di Sarra, A. G., Evangelisti, F., Duchi, R., Facchini, M. C., Fuzzi, S., Gobbi, G. P., Maione, M., Panday, A.,
295 Roccato, F., Sellegri, K., Venzac, H., Verza, G. P., Villani, P., Vuillermoz, E., and Cristofanelli, P.: Atmospheric Brown Clouds
296 in the Himalayas: first two years of continuous observations at the Nepal Climate Observatory-Pyramid (5079 m), Atmos.
297 Chem. Phys., 10, 7515-7531, 10.5194/acp-10-7515-2010, 2010.

298 Bougiatioti, A., Stavroulas, I., Kostenidou, E., Zarmpas, P., Theodosi, C., Kouvarakis, G., Canonaco, F., Prévôt, A. S. H.,
299 Nenes, A., Pandis, S. N., and Mihalopoulos, N.: Processing of biomass-burning aerosol in the eastern Mediterranean during
300 summertime, Atmos. Chem. Phys., 14, 4793-4807, 10.5194/acp-14-4793-2014, 2014.

301 Brito, J., Rizzo, L. V., Morgan, W. T., Coe, H., Johnson, B., Haywood, J., Longo, K., Freitas, S., Andreae, M. O., and Artaxo,
302 P.: Ground-based aerosol characterization during the South American Biomass Burning Analysis (SAMBBA) field experiment,
303 Atmos. Chem. Phys., 14, 12069-12083, 10.5194/acp-14-12069-2014, 2014.

304 Canagaratna, M. R., Jayne, J. T., Jimenez, J. L., Allan, J. D., Alfarra, M. R., Zhang, Q., Onasch, T. B., Drewnick, F., Coe, H.,
305 Middlebrook, A., Delia, A., Williams, L. R., Trimborn, A. M., Northway, M. J., DeCarlo, P. F., Kolb, C. E., Davidovits, P., and
306 Worsnop, D. R.: Chemical and microphysical characterization of ambient aerosols with the aerodyne aerosol mass spectrometer,
307 Mass Spectrom. Rev., 26, 185-222, 10.1002/mas.20115, 2007.

308 Canagaratna, M. R., Jimenez, J. L., Kroll, J. H., Chen, Q., Kessler, S. H., Massoli, P., Ruiz, L. H., Fortner, E., R.Williams, L.,
309 R.Wilson, K., Surratt, J. D., Donahue, N. M., Jayne, J. T., and R.Worsnop, D.: Elemental ratio measurements of organic
310 compounds using aerosol mass spectrometry: characterization, improved calibration, and implications, Atmospheric
311 Chemistry and Physics, 15, 253–272, 10.5194/acp-15-253-2015, 2015.

312 Cong, Z., Kang, S., Kawamura, K., Liu, B., Wan, X., Wang, Z., Gao, S., and Fu, P.: Carbonaceous aerosols on the south edge
313 of the Tibetan Plateau: concentrations, seasonality and sources, Atmos. Chem. Phys., 15, 1573-1584, 10.5194/acp-15-1573-
314 2015, 2015a.

315 Cong, Z., Kawamura, K., Kang, S., and Fu, P.: Penetration of biomass-burning emissions from South Asia through the
316 Himalayas: new insights from atmospheric organic acids, Sci. Rep., 5, 9580, 10.1038/srep09580, 2015b.

317 Crippa, M., DeCarlo, P. F., Slowik, J. G., Mohr, C., Heringa, M. F., Chirico, R., Poulain, L., Freutel, F., Sciare, J., Cozic, J., Di
318 Marco, C. F., Elsasser, M., Nicolas, J. B., Marchand, N., Abidi, E., Wiedensohler, A., Drewnick, F., Schneider, J., Borrmann,
319 S., Nemitz, E., Zimmermann, R., Jaffrezo, J. L., Prevot, A. S. H., and Baltensperger, U.: Wintertime aerosol chemical
320 composition and source apportionment of the organic fraction in the metropolitan area of Paris, Atmospheric Chemistry and
321 Physics, 13, 961-981, 10.5194/acp-13-961-2013, 2013.

322 Cubison, M. J., Ortega, A. M., Hayes, P. L., Farmer, D. K., Day, D., Lechner, M. J., Brune, W. H., Apel, E., Diskin, G. S.,
323 Fisher, J. A., Fuelberg, H. E., Hecobian, A., Knapp, D. J., Mikoviny, T., Riemer, D., Sachse, G. W., Sessions, W., Weber, R. J.,
324 Weinheimer, A. J., Wisthaler, A., and Jimenez, J. L.: Effects of aging on organic aerosol from open biomass burning smoke in

325 aircraft and laboratory studies, Atmospheric Chemistry and Physics, 11, 12049-12064, 10.5194/acp-11-12049-2011, 2011.

326 Decesari, S., Facchini, M. C., Carbone, C., Giulianelli, L., Rinaldi, M., Finessi, E., Fuzzi, S., Marinoni, A., Cristofanelli, P.,
327 Duchi, R., Bonasoni, P., Vuillermoz, E., Cozic, J., Jaffrezo, J. L., and Laj, P.: Chemical composition of PM_{10} and PM_1 at the
328 high-altitude Himalayan station Nepal Climate Observatory-Pyramid (NCO-P) (5079 m a.s.l.), Atmos. Chem. Phys., 10, 4583-
329 4596, 10.5194/acp-10-4583-2010, 2010.

330 Du, W., Sun, Y. L., Xu, Y. S., Jiang, Q., Wang, Q. Q., Yang, W., Wang, F., Bai, Z. P., Zhao, X. D., and Yang, Y. C.: Chemical
331 characterization of submicron aerosol and particle growth events at a national background site (3295 m a.s.l.) on the Tibetan
332 Plateau, Atmospheric Chemistry and Physics, 15, 10811-10824, 10.5194/acp-15-10811-2015, 2015.

333 Engling, G., and Gelencser, A.: Atmospheric Brown Clouds: From Local Air Pollution to Climate Change, Elements, 6, 223-
334 228, 10.2113/gselements.6.4.223, 2010.

335 Engling, G., Zhang, Y.-N., Chan, C.-Y., Sang, X.-F., Lin, M., Ho, K.-F., Li, Y.-S., Lin, C.-Y., and Lee, J. J.: Characterization
336 and sources of aerosol particles over the southeastern Tibetan Plateau during the Southeast Asia biomass-burning season,
337 Tellus B, 63, 117-128, 10.1111/j.1600-0889.2010.00512.x, 2011.

338 Fröhlich, R., Cubison, M. J., Slowik, J. G., Bukowiecki, N., Canonaco, F., Croteau, P. L., Gysel, M., Henne, S., Herrmann, E.,
339 Jayne, J. T., Steinbacher, M., Worsnop, D. R., Baltensperger, U., and Prévôt, A. S. H.: Fourteen months of on-line
340 measurements of the non-refractory submicron aerosol at the Jungfraujoch (3580 m a.s.l.) – chemical composition, origins and
341 organic aerosol sources, Atmospheric Chemistry and Physics, 15, 11373-11398, 10.5194/acp-15-11373-2015, 2015.

342 Freney, E. J., Sellegri, K., Canonaco, F., Boulon, J., Hervo, M., Weigel, R., Pichon, J. M., Colomb, A., Prévôt, A. S. H., and
343 Laj, P.: Seasonal variations in aerosol particle composition at the puy-de-Dôme research station in France, Atmos. Chem. Phys.,
344 11, 13047-13059, 10.5194/acp-11-13047-2011, 2011.

345 He, L. Y., Lin, Y., Huang, X. F., Guo, S., Xue, L., Su, Q., Hu, M., Luan, S. J., and Zhang, Y. H.: Characterization of high-
346 resolution aerosol mass spectra of primary organic aerosol emissions from Chinese cooking and biomass burning, Atmospheric
347 Chemistry and Physics, 10, 11535-11543, 10.5194/acp-10-11535-2010, 2010.

348 Hu, W. W., Hu, M., Yuan, B., Jimenez, J. L., Tang, Q., Peng, J. F., Hu, W., Shao, M., Wang, M., Zeng, L. M., Wu, Y. S., Gong,
349 Z. H., Huang, X. F., and He, L. Y.: Insights on organic aerosol aging and the influence of coal combustion at a regional receptor
350 site of central eastern China, Atmospheric Chemistry and Physics, 13, 10095-10112, 10.5194/acp-13-10095-2013, 2013.

351 Hu, W. W., Hu, M., Hu, W., Jimenez, J. L., Yuan, B., Chen, W. T., Wang, M., Wu, Y. S., Chen, C., Wang, Z. B., Peng, J. F.,
352 Zeng, L. M., and Shao, M.: Chemical composition, sources, and aging process of submicron aerosols in Beijing: Contrast
353 between summer and winter, JGRD, 121, 1955-1977, 10.1002/2015jd024020, 2016.

354 Huang, X.-F., Xue, L., Tian, X.-D., Shao, W.-W., Sun, T.-L., Gong, Z.-H., Ju, W.-W., Jiang, B., Hu, M., and He, L.-Y.: Highly
355 time-resolved carbonaceous aerosol characterization in Yangtze River Delta of China: Composition, mixing state and
356 secondary formation, Atmos. Environ., 64, 200-207, 10.1016/j.atmosenv.2012.09.059, 2013.

357 Huang, X. F., He, L. Y., Hu, M., Canagaratna, M. R., Sun, Y., Zhang, Q., Zhu, T., Xue, L., Zeng, L. W., Liu, X. G., Zhang, Y.
358 H., Jayne, J. T., Ng, N. L., and Worsnop, D. R.: Highly time-resolved chemical characterization of atmospheric submicron
359 particles during 2008 Beijing Olympic Games using an Aerodyne High-Resolution Aerosol Mass Spectrometer, Atmospheric

Chemistry and Physics, 10, 8933-8945, 10.5194/acp-10-8933-2010, 2010.

Huang, X. F., He, L. Y., Hu, M., Canagaratna, M. R., Kroll, J. H., Ng, N. L., Zhang, Y. H., Lin, Y., Xue, L., Sun, T. L., Liu, X. G., Shao, M., Jayne, J. T., and Worsnop, D. R.: Characterization of submicron aerosols at a rural site in Pearl River Delta of China using an Aerodyne High-Resolution Aerosol Mass Spectrometer, Atmospheric Chemistry and Physics, 11, 1865-1877, 10.5194/acp-11-1865-2011, 2011.

Huang, X. F., He, L. Y., Xue, L., Sun, T. L., Zeng, L. W., Gong, Z. H., Hu, M., and Zhu, T.: Highly time-resolved chemical characterization of atmospheric fine particles during 2010 Shanghai World Expo, Atmospheric Chemistry and Physics, 12, 4897-4907, 10.5194/acp-12-4897-2012, 2012.

IPCC: Climate change: the physical science basis, Cambridge University Press, Cambridge, England, 2013.

Jimenez, J. L., Canagaratna, M. R., Donahue, N. M., Prevot, A. S. H., Zhang, Q., Kroll, J. H., DeCarlo, P. F., Allan, J. D., Coe, H., Ng, N. L., Aiken, A. C., Docherty, K. S., Ulbrich, I. M., Grieshop, A. P., Robinson, A. L., Duplissy, J., Smith, J. D., Wilson, K. R., Lanz, V. A., Hueglin, C., Sun, Y. L., Tian, J., Laaksonen, A., Raatikainen, T., Rautiainen, J., Vaattovaara, P., Ehn, M., Kulmala, M., Tomlinson, J. M., Collins, D. R., Cubison, M. J., Dunlea, J., Huffman, J. A., Onasch, T. B., Alfarra, M. R., Williams, P. I., Bower, K., Kondo, Y., Schneider, J., Drewnick, F., Borrmann, S., Weimer, S., Demerjian, K., Salcedo, D., Cottrell, L., Griffin, R., Takami, A., Miyoshi, T., Hatakeyama, S., Shimono, A., Sun, J. Y., Zhang, Y. M., Dzepina, K., Kimmel, J. R., Sueper, D., Jayne, J. T., Herndon, S. C., Trimborn, A. M., Williams, L. R., Wood, E. C., Middlebrook, A. M., Kolb, C. E., Baltensperger, U., and Worsnop, D. R.: Evolution of Organic Aerosols in the Atmosphere, Science, 326, 1525-1529, 10.1126/science.1180353, 2009.

Jolleys, M. D., Coe, H., McFiggans, G., Taylor, J. W., O'Shea, S. J., Breton, M. L., Bauguitte, S. J.-B., Moller, S., Carlo, P. D., Aruffo, E., Palmer, P. I., Lee, J. D., Percival, C. J., and Gallagher, M. W.: Properties and evolution of biomass burning organic aerosol from Canadian boreal forest fire, Atmos. Chem. Phys., 15, 3077-3095, 10.5194/acp-15-3077-2015, 2015.

Lüthi, Z. L., Škerlak, B., Kim, S. W., Lauer, A., Mues, A., Rupakheti, M., and Kang, S.: Atmospheric brown clouds reach the Tibetan Plateau by crossing the Himalayas, Atmos. Chem. Phys., 15, 6007-6021, 10.5194/acp-15-6007-2015, 2015.

Lau, W. K. M., Kim, M.-K., Kim, K.-M., and Lee, W.-S.: Enhanced surface warming and accelerated snow melt in the Himalayas and Tibetan Plateau induced by absorbing aerosols, Environ. Res. Lett., 5, 025204, 10.1088/1748-9326/5/2/025204, 2010.

Li, Y. J., Lee, B. P., Su, L., Fung, J. C. H., and Chan, C. K.: Seasonal characteristics of fine particulate matter (PM) based on high-resolution time-of-flight aerosol mass spectrometric HR-ToF-AMS) measurements at the HKUST Supersite in Hong Kong, Atmospheric Chemistry and Physics, 15, 37–53, 10.5194/acp-15-37-2015, 2015.

Marinoni, A., Cristofanelli, P., Laj, P., Duchi, R., Calzolari, F., Decesari, S., Sellegri, K., Vuillermoz, E., Verza, G. P., Villani, P., and Bonasoni, P.: Aerosol mass and black carbon concentrations, a two year record at NCO-P (5079 m, Southern Himalayas), Atmos. Chem. Phys., 10, 8551-8562, 10.5194/acp-10-8551-2010, 2010.

Middlebrook, A. M., Bahreini, R., Jimenez, J. L., and Canagaratna, M. R.: Evaluation of Composition-Dependent Collection Efficiencies for the Aerodyne Aerosol Mass Spectrometer using Field Data, Aerosol Sci. Technol., 46, 258-271, 10.1080/02786826.2011.620041, 2012.

Ming, J., Xiao, C., Sun, J., Kang, S., and Bonasoni, P.: Carbonaceous particles in the atmosphere and precipitation of the Nam Co region, central Tibet, J. Environ. Sci., 22, 1748-1756, 10.1016/s1001-0742(09)60315-6, 2010.

Minguillón, M. C., Ripoll, A., Pérez, N., Prévôt, A. S. H., Canonaco, F., Querol, X., and Alastuey, A.: Chemical characterization of submicron regional background aerosols in the western Mediterranean using an Aerosol Chemical Speciation Monitor, Atmospheric Chemistry and Physics, 15, 6379-6391, 10.5194/acp-15-6379-2015, 2015.

Ng, N. L., Canagaratna, M. R., Zhang, Q., Jimenez, J. L., Tian, J., Ulbrich, I. M., Kroll, J. H., Docherty, K. S., Chhabra, P. S., Bahreini, R., Murphy, S. M., Seinfeld, J. H., Hildebrandt, L., Donahue, N. M., DeCarlo, P. F., Lanz, V. A., Prévôt, A. S. H., Dinar, E., Rudich, Y., and Worsnop, D. R.: Organic aerosol components observed in Northern Hemispheric datasets from Aerosol Mass Spectrometry, Atmospheric Chemistry and Physics, 10, 4625-4641, 10.5194/acp-10-4625-2010, 2010.

Paatero, P., and Tapper, U.: Positive matrix factorization: A non-negative factor model with optimal utilization of error estimates of data values, Environmetrics, 5, 111-126, 10.1002/env.3170050203, 1994.

Qian, Y., Flanner, M. G., Leung, L. R., and Wang, W.: Sensitivity studies on the impacts of Tibetan Plateau snowpack pollution on the Asian hydrological cycle and monsoon climate, Atmos. Chem. Phys., 11, 1929-1948, 10.5194/acp-11-1929-2011, 2011.

Ripoll, A., Minguillón, M. C., Pey, J., Jimenez, J. L., Day, D. A., Sosedova, Y., Canonaco, F., Prévôt, A. S. H., Querol, X., and Alastuey, A.: Long-term real-time chemical characterization of submicron aerosols at Montsec (southern Pyrenees, 1570ma.s.l.), Atmos. Chem. Phys., 15, 2935–2951, 10.5194/acp-15-2935-2015, 2015.

Sjogren, S., Gysel, M., E.Weingartner, Alfarra, M. R., Duplissy, J., Cozic, J., Crosier, J., Coe, H., and Baltensperger, U.: Hygroscopicity of the submicrometer aerosol at the high-alpine site Jungfraujoch, 3580m a.s.l., Switzerland, Atmos. Chem. Phys., 8, 5715–5729, 10.5194/acp-8-5715-2008, 2008.

Streets, D. G., Yarber, K. F., Woo, J. H., and Carmichael, G. R.: Biomass burning in Asia: Annual and seasonal estimates and atmospheric emissions, Global Biogeochem. Cycles, 17, 1759-1768, 10.1029/2003gb002040, 2003.

Sun, Y. L., Zhang, Q., Schwab, J. J., Demerjian, K. L., Chen, W. N., Bae, M. S., Hung, H. M., Hogrefe, O., Frank, B., Rattigan, O. V., and Lin, Y. C.: Characterization of the sources and processes of organic and inorganic aerosols in New York city with a high-resolution time-of-flight aerosol mass apectrometer, Atmospheric Chemistry and Physics, 11, 1581-1602, 10.5194/acp-11-1581-2011, 2011.

Ulbrich, I. M., Canagaratna, M. R., Zhang, Q., Worsnop, D. R., and Jimenez, J. L.: Interpretation of organic components from Positive Matrix Factorization of aerosol mass spectrometric data, Atmospheric Chemistry and Physics, 9, 2891-2918, 10.5194/acp-9-2891-2009, 2009.

von Schneidemesser, E., Monks, P. S., Allan, J. D., Bruhwiler, L., Forster, P., Fowler, D., Lauer, A., Morgan, W. T., Paasonen, P., Righi, M., Sindelarova, K., and Sutton, M. A.: Chemistry and the Linkages between Air Quality and Climate Change, Chem. Rev., 115, 3856-3897, 10.1021/acs.chemrev.5b00089, 2015.

Wan, X., Kang, S., Wang, Y., Xin, J., Liu, B., Guo, Y., Wen, T., Zhang, G., and Cong, Z.: Size distribution of carbonaceous aerosols at a high-altitude site on the central Tibetan Plateau (Nam Co Station, 4730ma.s.l.), Atmos. Res., 153, 155-164, 10.1016/j.atmosres.2014.08.008, 2015.

Wang, B., and French, H. M.: Climate Controls and High-Altitude Permafrost, Qinghai-Xizang (Tibet) Plateau, China,

430 Permafrost and Periglacial Processes, 5, 87-100, 10.1002/ppp.3430050203, 1994.

431 Wang, B., Liu, Y., Shao, M., Lu, S., Wang, M., Yuan, B., Gong, Z., He, L., Zeng, L., Hu, M., and Zhang, Y.: The contributions

432 of biomass burning to primary and secondary organics: A case study in Pearl River Delta (PRD), China, Sci. Total. Environ.,

433 569-570, 548-556, 10.1016/j.scitotenv.2016.06.153, 2016.

434 Xia, X., Zong, X., Cong, Z., Chen, H., Kang, S., and Wang, P.: Baseline continental aerosol over the central Tibetan plateau

435 and a case study of aerosol transport from South Asia, Atmos. Environ., 45, 7370-7378, 10.1016/j.atmosenv.2011.07.067, 2011.

436 Xu, J., Zhang, Q., Li, X., Ge, X., Xiao, C., Ren, J., and Qin, D.: Dissolved organic matter and inorganic ions in a central

437 Himalayan glacier--insights into chemical composition and atmospheric sources, Environ. Sci. Technol., 47, 6181-6188,

438 10.1021/es4009882, 2013.

439 Xu, J., Wang, Z., Yu, G., Qin, X., Ren, J., and Qin, D.: Characteristics of water soluble ionic species in fine particles from a

440 high altitude site on the northern boundary of Tibetan Plateau: Mixture of mineral dust and anthropogenic aerosol, Atmos.

441 Res., 143, 43-56, 10.1016/j.atmosres.2014.01.018, 2014a.

442 Xu, J., Zhang, Q., Chen, M., Ge, X., Ren, J., and Qin, D.: Chemical composition, sources, and processes of urban aerosols

443 during summertime in northwest China: insights from high-resolution aerosol mass spectrometry, Atmospheric Chemistry and

444 Physics, 14, 12593-12611, 10.5194/acp-14-12593-2014, 2014b.

445 Xu, J. Z., Zhang, Q., Wang, Z. B., Yu, G. M., Ge, X. L., and Qin, X.: Chemical composition and size distribution of summertime

446 $PM_{2.5}$ at a high altitude remote location in the northeast of the Qinghai–Xizang (Tibet) Plateau: insights into aerosol sources

447 and processing in free troposphere, Atmospheric Chemistry and Physics, 15, 5069-5081, 10.5194/acp-15-5069-2015, 2015.

448 You, C., Xu, C., Xu, B., Zhao, H., and Song, L.: Levoglucosan evidence for biomass burning records over Tibetan glaciers,

449 Environ. Pollu., 216, 173-181, 10.1016/j.envpol.2016.05.074, 2016.

450 Zhang, Q., Jimenez, J. L., Canagaratna, M. R., Ulbrich, I. M., Ng, N. L., Worsnop, D. R., and Sun, Y.: Understanding

451 atmospheric organic aerosols via factor analysis of aerosol mass spectrometry: a review, Anal Bioanal Chem, 401, 3045-3067,

452 10.1007/s00216-011-5355-y, 2011.

453 Zhang, Y., Tang, L., Wang, Z., Yu, H. X., Sun, Y. L., Liu, D., Qin, W., Canonaco, F., Prévôt, A. S. H., Zhang, H. L., and Zhou,

454 H. C.: Insights into characteristics, sources, and evolution of submicron aerosols during harvest seasons in the Yangtze River

455 delta region, China, Atmospheric Chemistry and Physics, 15, 1331-1349, 10.5194/acp-15-1331-2015, 2015.

456 Zhao, Z., Cao, J., Shen, Z., Xu, B., Zhu, C., Chen, L. W. A., Su, X., Liu, S., Han, Y., Wang, G., and Ho, K.: Aerosol particles

457 at a high-altitude site on the Southeast Tibetan Plateau, China: Implications for pollution transport from South Asia, J. Geophys.

458 Res. Atmos, 118, 11,360-311,375, 10.1002/jgrd.50599, 2013.

459

460

461

462

463

Table 1. Comparison between mass spectra of different OA with reference spectra.

	Reference spectra	Pearson Correlation Coefficient (N=100)			Citation
		BBOA	OOA-BB	OOA	
Ambient measurement	900m above fire	0.91	0.56	0.34	Brito et al. (2014)
	3h downwind	0.51	0.97	0.91	Brito et al. (2014)
	MO-OOA	0.69	0.86	0.69	Hu et al. (2016)
	BBOA	0.85	0.38	0.11	Hu et al. (2016)
Laboratory simulation	wood of pin	0.91	0.61	0.42	He et al. (2010)
	rice straw	0.94	0.6	0.36	He et al. (2010)

464

465

466

467

468

469

470

471

472
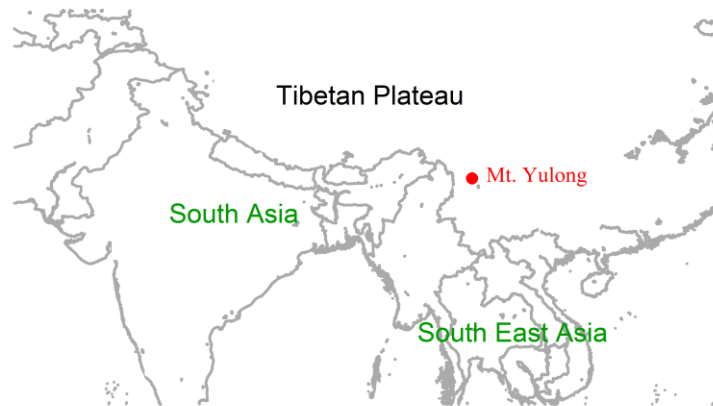
473 **Figure 1.** The location of the sampling site at Mt. Yulong (27.2 °N 100.2 °E, 3410 m a.s.l.).

474

475
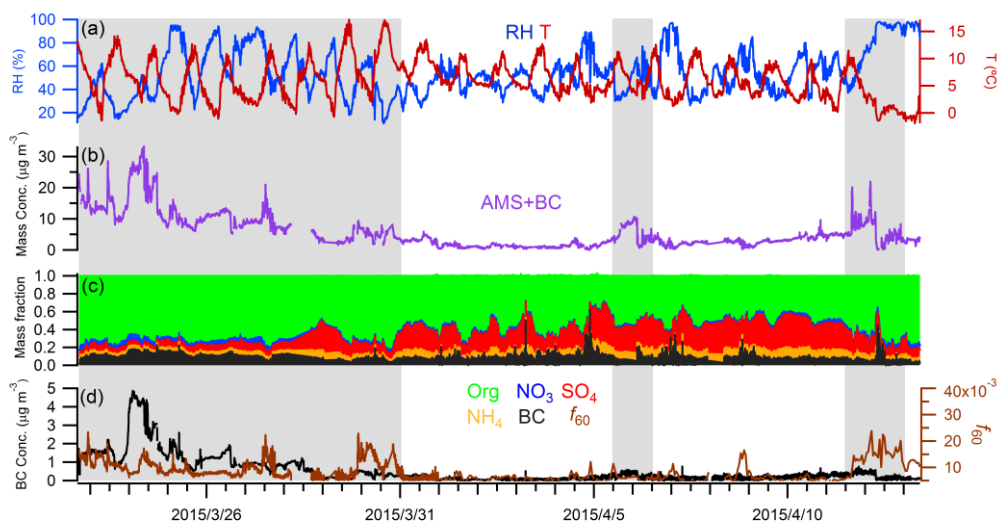
476 **Figure 2.** Time series of (a) relative humidity and temperature; (b) total mass concentrations from AMS plus black carbon (c) mass

477 fractions of different chemical species; (d) concentrations of black carbon and f_{60}. The gray background denotes three biomass burning
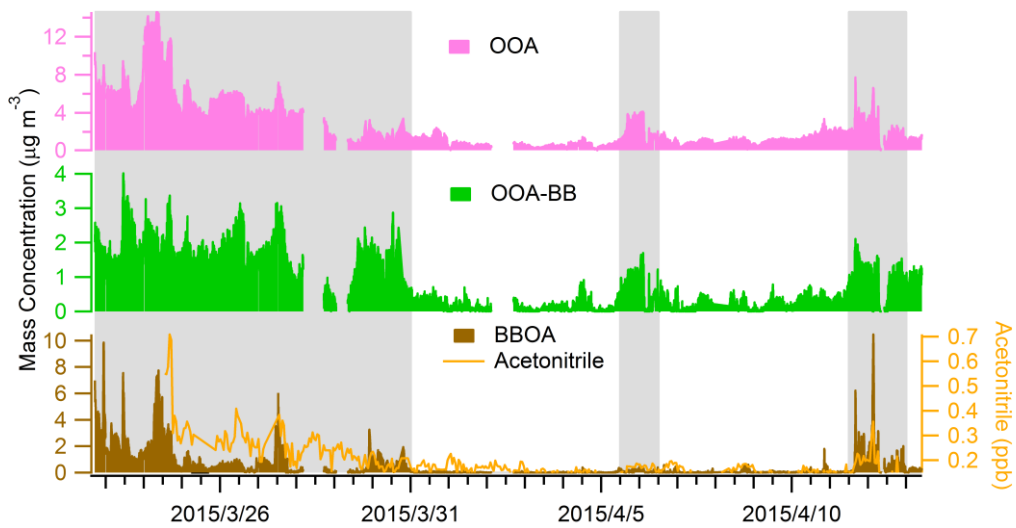
478 events (identified in Sect. 4.1).

479

480 **Figure 3.** (a) average chemical composition of the whole campaign; (b) the mass fractions of PM_1 species as a function of PM_1 mass

481 loading (left axis), with the white line representing the probability density of PM_1 mass loadings (right axis); (c) the diel cycle of different

482 species, with the left axis for organics, and the right axis for the rest components.
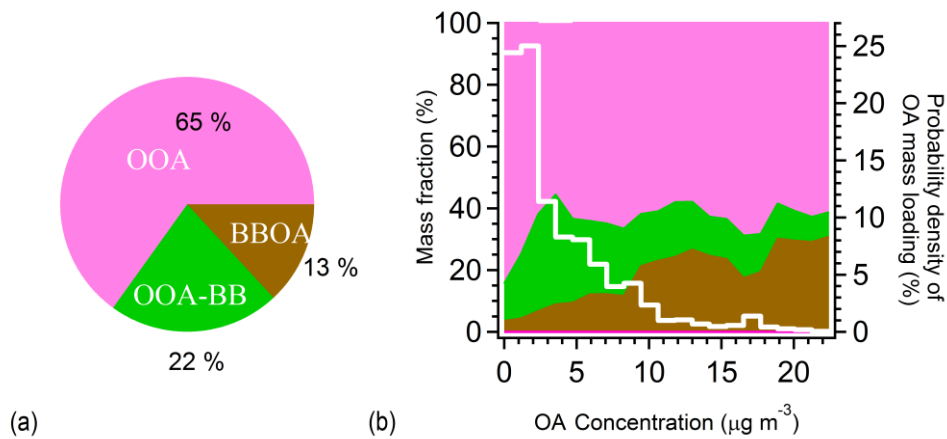
483
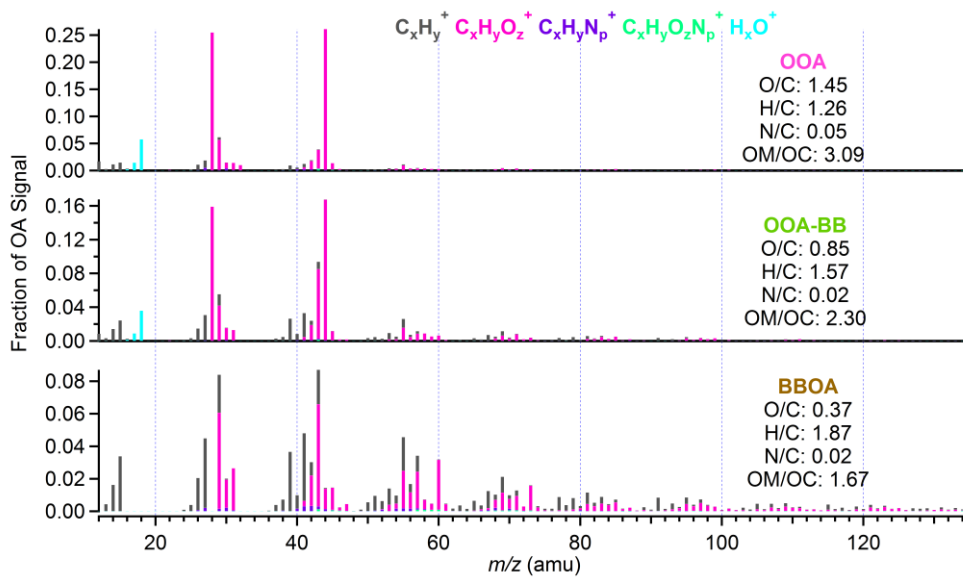
484

485 **Figure 4.** The mass spectra of each factor resolved by PMF, together with atomic ratios of each factor.

21

Figure 5. The time series of three OA factors resolved by PMF, together with acetonitrile. The grey background areas denote the

biomass burning events (identified in Sect. 4.1).

(a)   (b)

Figure 6. (a) contribution of each factor to the total OA mass; (b) fractions of OA factor (left axis) and probability density of OA

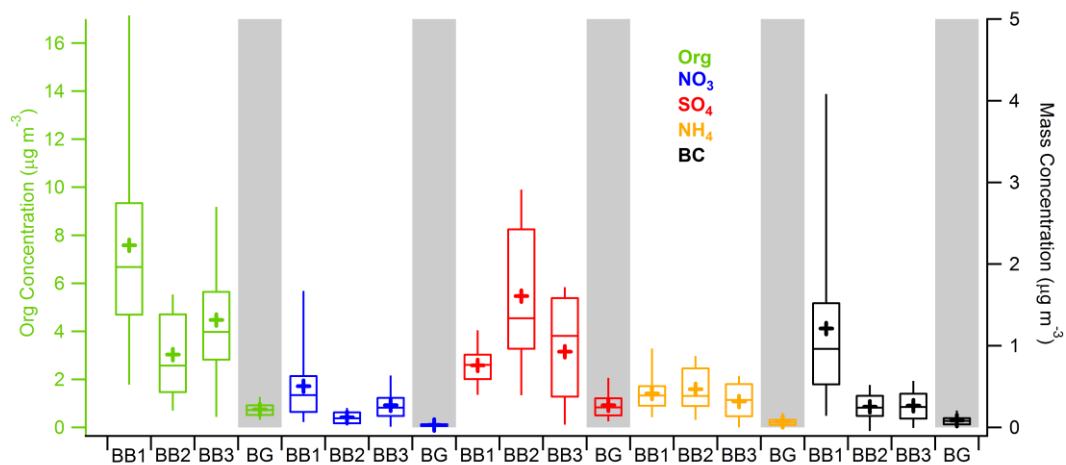concentration (white line, right axis) as a function of OA mass loading.

492
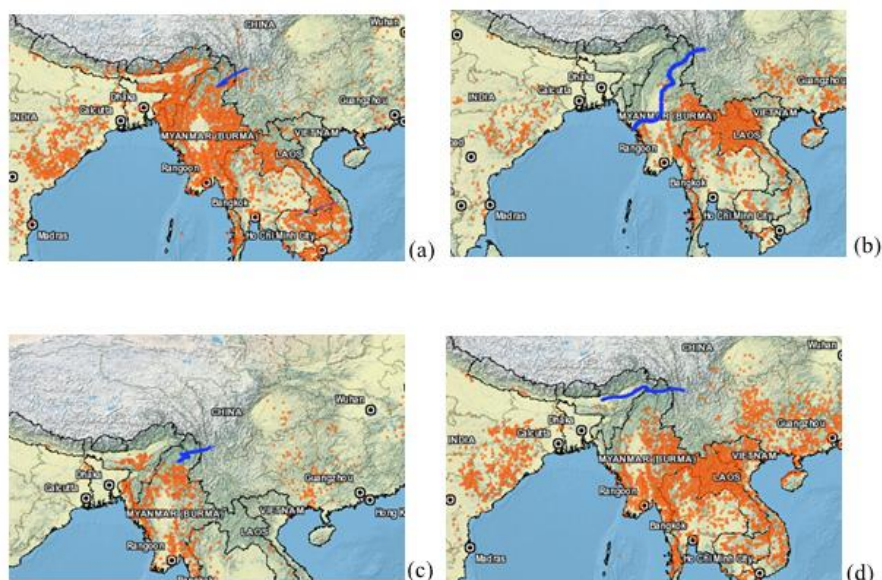
Figure 7. Occurrence of wildfire derived from MODIS images and back trajectories (blue lines) from WRF model (a) first biomass

burning event: March 22nd–30th; (b) second biomass burning event: April 5th–6th; (c) third biomass burning event: April 11th–12th; (d)

background: April 1st–4th.

496   **Figure 8.** Comparison of chemical compositions between three biomass burning events (BB1, BB2, BB3) and background conditions

23

497   (BG, highlighted by light gray color). Boxes denote median, 25th and 75th percentiles; whiskers represent 5th and 95th percentiles; crosses

498   represent mean values. Organic aerosols are represented by the left axis while other species are represented by the right axis.

499
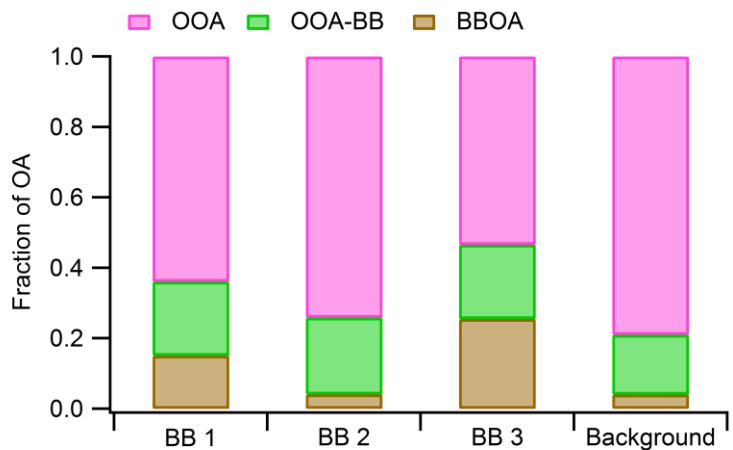
500
501   **Figure 9.** The relative contribution of different types of OA during three biomass burning events and background condition.
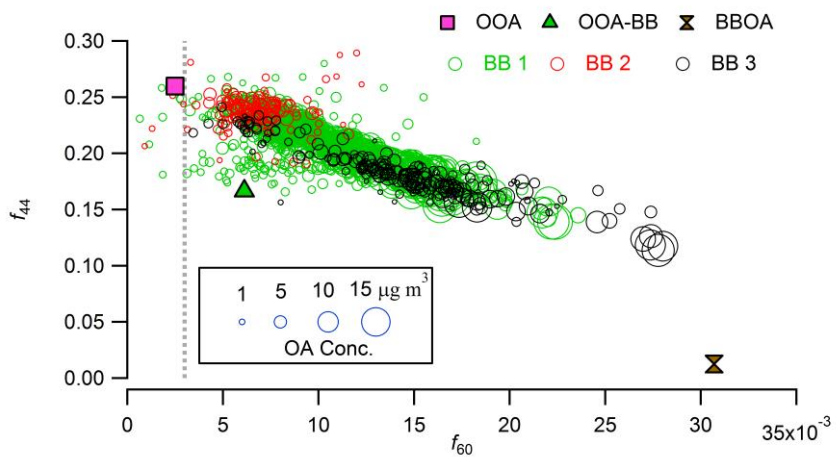
502

503   **Figure 10.** f_{44} as a function of f_{60} (f_{44} vs. f_{60} triangle plot) of the three biomass burning events, sized by OA concentration.